THE PROTEIN SOCIETY

Mycobacterium tuberculosis RpfE crystal structure reveals a positively charged catalytic cleft

Daniela Mavrici, Daniil M. Prigozhin, and Tom Alber*

Department of Molecular and Cell Biology and California Institute for Quantitative Biosciences, University of California, Berkeley, California 94720

Received 6 December 2013; Accepted 17 January 2014
DOI: 10.1002/pro.2431
Published online 22 January 2014 proteinscience.org

Tom Alber is the recipient of the 2013 Protein Society Christian B. Anfinsen Award

Abstract: Resuscitation promoting factor (Rpf) proteins, which hydrolyze the sugar chains in cell-wall peptidoglycan (PG), play key roles in prokaryotic cell elongation, division, and escape from dormancy to vegetative growth. Like other bacteria, *Mycobacterium tuberculosis* (*Mtb*) expresses multiple Rpfs, none of which is individually essential. This redundancy has left unclear the distinct functions of the different Rpfs. To explore the distinguishing characteristics of the five *Mtb* Rpfs, we determined the crystal structure of the RpfE catalytic domain. The protein adopts the characteristic Rpf fold, but the catalytic cleft is narrower compared to *Mtb* RpfB. Also in contrast to RpfB, in which the substrate-binding surfaces are negatively charged, the corresponding RpfE catalytic pocket and predicted peptide-binding sites are more positively charged at neutral pH. The complete reversal of the electrostatic potential of the substrate-binding site suggests that the different Rpfs function optimally at different pHs or most efficiently hydrolyze different micro-domains of PG. These studies provide insights into the molecular determinants of the evolution of functional specialization in Rpfs.

Keywords: resuscitation promoting factor; lytic transglycosylase; peptidoglycan hydrolase; enzyme specificity; electrostatic complementarity

Introduction

It has been estimated that one-third of world population is infected by *Mycobacterium tuberculosis* (*Mtb*). In most infected individuals, *Mtb* persists in a latent state for years until host conditions favor reactivation.[1,2] A family of enzymes, called resuscitation promoting factors (Rpfs), plays a central role in *Mtb* reactivation.[2–4] Rpfs share a lytic-transglycosylase domain[5–7] that hydrolyzes the glycan chains in the peptidoglycan (PG) sugar-peptide meshwork that surrounds every bacterial cell and protects it against environmental stresses. Additionally, Rpf proteins are thought to collaborate in releasing a PG fragment that binds the sensor domain of PknB and signals the transition from dormancy to vegetative growth.[8,9] During growth, the catalytic activity of Rpfs is crucial for cell elongation and division.[10,11]

Mtb encodes five Rpf proteins (Rv0867c, Rv1009, Rv1884c, Rv2389c, and Rv2450c named RpfA-E).[12] They are generally predicted to be secreted (RpfA,B,E) or anchored to the membrane (RpfD). RpfA, C, and E contain low-complexity segments that are expected to be unfolded. Among the

Abbreviations: Mtb, *Mycobacterium tuberculosis*; NAG_3, *N,N′,N″*-triacetyl-chitotriose; PG, peptidoglycan; PDB, Protein Data Bank; Rpf, resuscitation promoting factor; RipA, Rpf-interacting protein A; RMSD, root-mean-square deviation

Grant sponsor: US National Institutes of Health; Grant number: P01AI095208.

*Correspondence to: Tom Alber, Department of Molecular and Cell Biology, California Institute of Quantitative Biosciences (QB3), University of California at Berkeley, 374B Stanley Hall, Berkeley, CA 94720. E-mail: tom@ucxray.berkeley.edu

five Rpfs, only RpfB contains additional domains, a predicted G5 cell-wall adhesive domain and a repetitive domain of unknown function (DUF348).[7]

The Rpfs appear to be functionally redundant, since deletion of each single gene causes no differences in cell growth or cell morphology in rich medium *in vitro*. Thus, no member of the family is essential for growth in culture.[13,14] The combined deletions of at least three *rpf* genes produce cell-growth defects *in vitro*, uncovering apparent functional specialization of Rpfs in *Mtb*.[13] Consistent with this idea, the *Mtb rpfB* deletion mutant fails to resuscitate in mice,[3] while *rpfE* is individually essential for switching mycobacterial cultures from slow to fast growth in a chemostat.[15] These results provide functional data suggesting that RpfB and RpfE are the most important Rpf family members.[9] To better understand the specialized roles of the *Mtb* Rpfs, we determined the crystal structure of the RpfE catalytic domain and compared the structure to RpfB.[7]

Results and Discussion

To obtain the soluble RpfE catalytic domain (residues 98–172), we deleted the predicted signal peptide (1–28) and low complexity region (28–97). The predicted catalytic domain (98–172) was expressed in *E. coli*, and the protein was exposed to 10:1 mixture of reduced to oxidized glutathione during the purification to form the disulfide bond conserved in this protein family. Purified RpfE crystallized readily in almost 70% of more than 500 conditions screened. Increasing the salt concentration from 0.1*M* to 0.3*M* and changing the pH failed to improve the crystal morphology. The best crystals for diffraction were obtained using an additive screen (Silver Bullets HT). The structure was determined by molecular replacement at 2.76 Å resolution (Table I) using the catalytic domain of RpfB (3EO5)[7] as the search model. The asymmetric unit contained 6 molecules, with a Cα RMSD of 0.336 Å. The model (R/R_{free} = 0.235/0.287) contains the entire sequence of each chain except for Ser98, Arg171, and Gly172 in chains A and C, Ser98, Ala144 in chain B, Ser98, Val99, Arg171 and Gly172 in chains D, E, and F.

Table I. *X-Ray Data Collection, Analysis, and Refinement Statistics for the Crystal Structure of the RpfE*

Data collection	
Space group	$P2_1$
Cell dimensions	
a, *b*, *c* (Å)	34.54 84.00 72.63
α, β, γ (°)	90, 103.53, 90
Wavelength	1.11
Resolution (Å)	42.0–2.756 (2.85–2.76)
No. reflections	10,478 (1021)
R_{merge} (%)	12.9% (81.9)
$I/\sigma I$	109.5/10.2 (13.9/6.9)
Completeness (%)	99.61 (96.32)
Redundancy	3.9 (3.8)
Refinement	
Resolution (Å)	36.0–2.76
R_{work}/R_{free}	0.235/0.287
No. atoms	3241
Protein	3234
Water	7
Protein residues	431
B-factors	49.30
Protein	49.30
Water	44.90
R.m.s. deviations	
Bond lengths (Å)	0.002
Bond angles (°)	0.58
Ramachandran plot	
Ramachandran favored (%)	93
Ramachandran outliers (%)	1.7
PDB ID	**4CGE**

Comparison between RpfE and RpfB catalytic domains

The RpfE catalytic domain adopts the fold of six alpha helices with a single disulfide bond as observed in RpfB[7] [Fig. 1(A)], which shares 64% sequence identity. The Cα RMSD between RpfB and the six molecules of the RpfE catalytic domain in the asymmetric unit ranges from 0.52 to 0.78 Å. The RpfE catalytic cleft contains the conserved Glu102 characteristic of lytic transglycosylases. These features suggest that RpfE and RpfB bind the substrates in similar orientation and catalyze hydrolysis by similar mechanisms.

Unlike RpfB, however, RpfE does not show the two short 3_{10} helices in the α2–α3 loop. In addition, the active site cleft of RpfE is 0.8–2.3 Å wider than the cleft in RpfB [Fig. 1(B)]. This expansion increases the surface and volume of the catalytic cleft (RpfE 122.5 Å^3, 95.8 Å^2 and RpfB 82.3 Å^3, 94.8 Å^2, respectively).

A third large difference between RpfE and RpfB is the calculated electrostatic potential of the surface of the catalytic cleft [Fig. 1(C)]. The RpfE catalytic domain is a basic protein (calculated pI = 9.5), compared to the acidic RpfB catalytic domain (calculated pI = 5.5). This sequence variation produces a dramatic difference in the calculated charge states of surface residues at neutral pH. In particular, charge differences occur on the surfaces in and around the active site. The pocket containing the catalytic glutamate, for example, is calculated to be negatively charged in RpfB and more neutral in RpfE [Fig. 1(C)]. This difference in the predicted p*K*a of the catalytic glutamate suggests that these enzymes may have different pH optima.

Specialization of substrate binding surfaces

In addition to the catalytic site, the predicted substrate binding surfaces differ in RpfE and RpfB. The structure of RpfB bound to the substrate analog

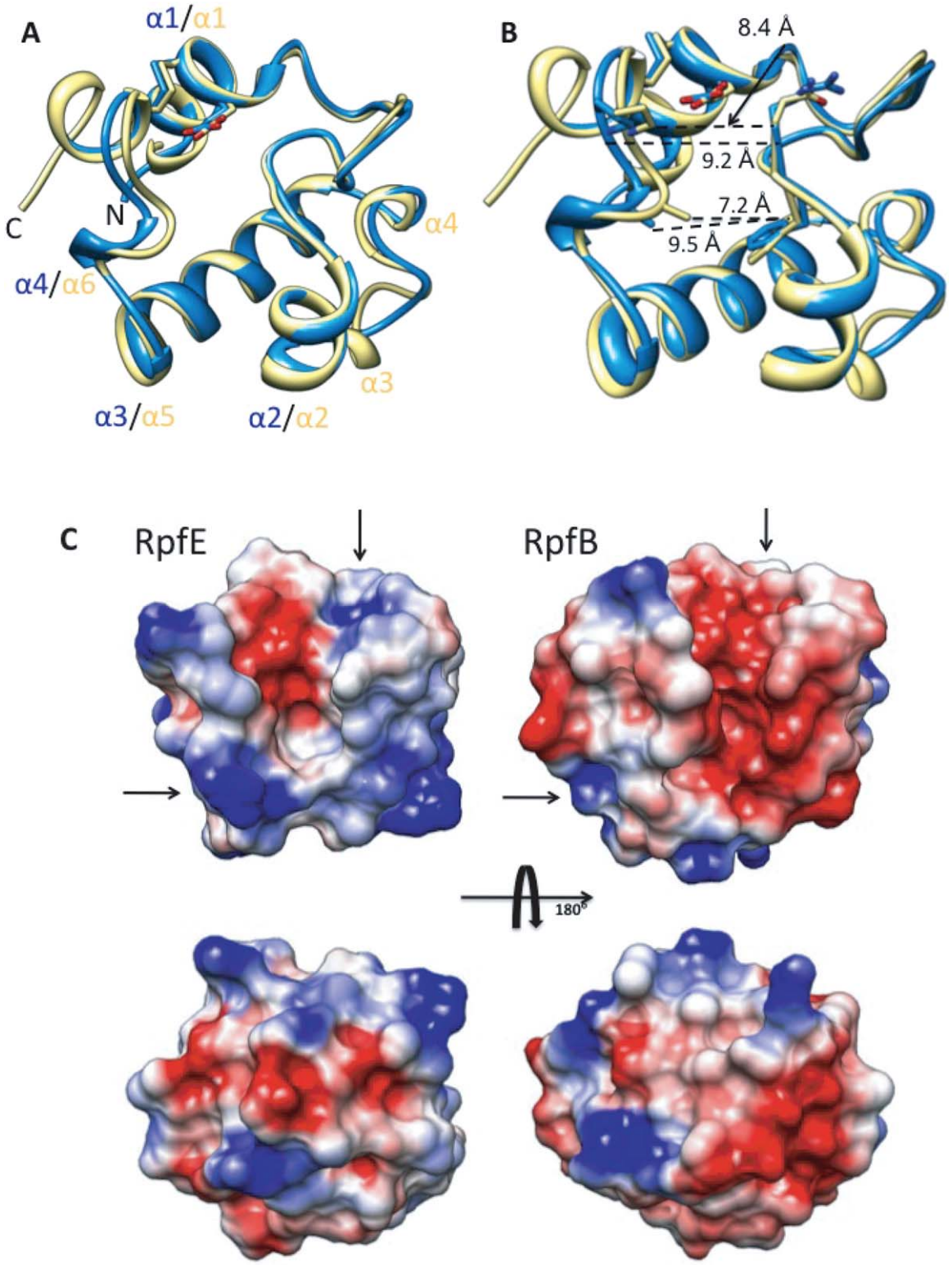

Figure 1. A: Ribbon representation of superimposed RpfE (blue) and RpfB (yellow) catalytic domain. The conserved, catalytic glutamate is shown in stick representation. B: RpfE and RpfB catalytic-cleft, Cα distance differences. C: Electrostatic potential surfaces (blue, $> +5$ kT and red, < -5 kT) of RpfE and RpfB calculated using the program Swiss-PdbViewer. RpfE shows positive potential around the predicted peptide-binding surfaces (arrows), while RpfB presents predicted peptide-binding surfaces (arrows) that are calculated to be negatively charged at neutral pH.

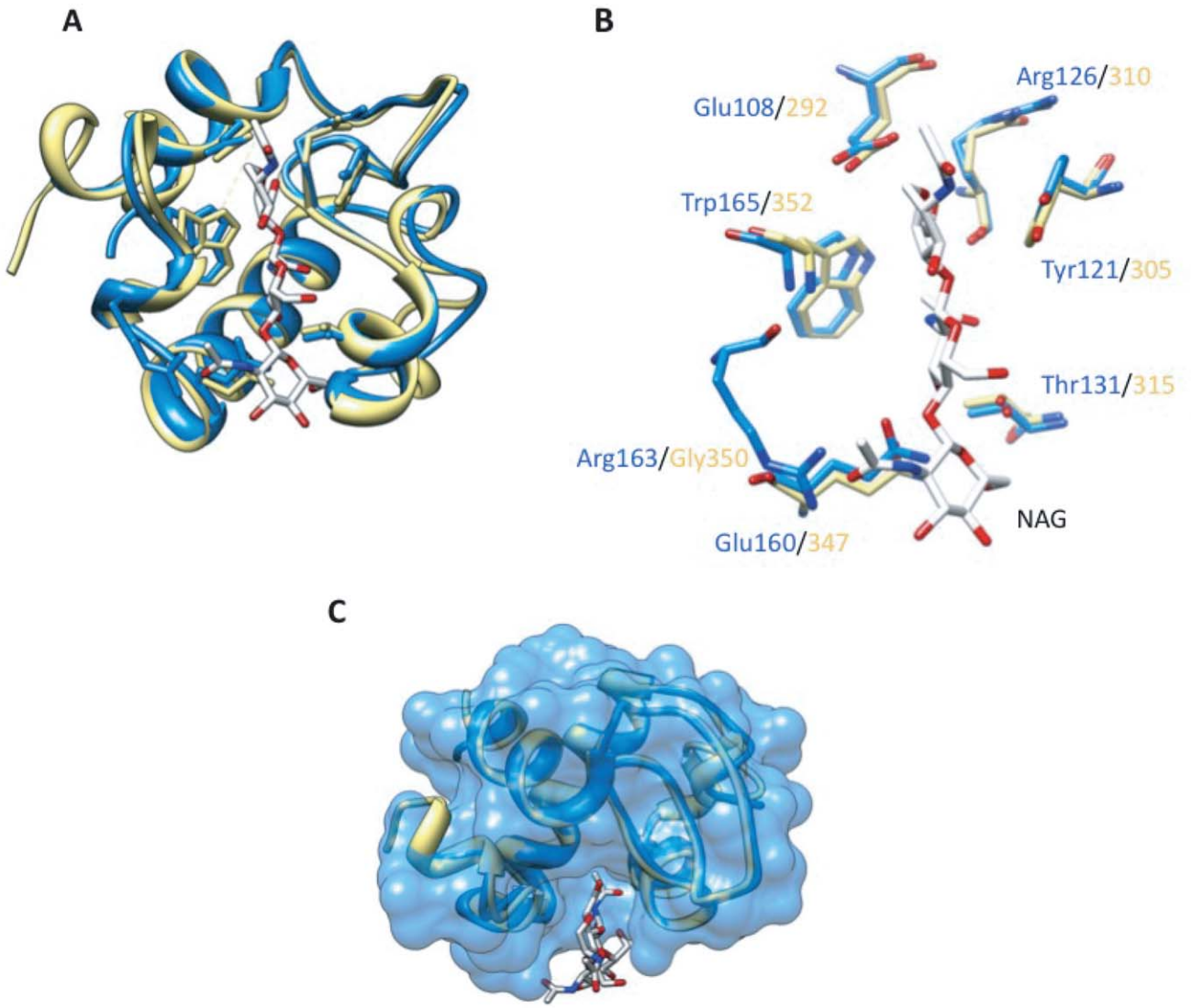

Figure 2. A: Superimposed RpfE (blue) and RpfB (yellow) catalytic domain bound to NAG_3. B: Superimposed RpfE (blue) and RpfB (yellow) residues in the catalytic cleft involved in binding NAG_3. All the residues are conserved between the two enzymes except for Gly350 substituted in RpfE by Arg163. C: RpfE surface with NAG_3 modeled in the catalytic cleft, based on a superposition with the structure of the RpfB-NAG_3 complex (PDB ID:4KPM). RpfE Arg163 overlaps with substrate, indicating that a conformational adjustment or a different ligand stereochemistry is necessary to accommodate the substrate in the catalytic cleft.

NAG_3 (**4KPM** in PDB)[16] supported modeling of the enzyme–substrate complex, which identified likely binding sites not only for the carbohydrate, but also for the peptide crosslinks in PG[16] [Fig. 2(A)]. The crosslinks differ in the identity of the second residue (isoglutamate or isoglutamine), the covalently bonded residues (3-4 or 3-3), cleavage of the terminal D-Ala, and other modifications.[17] Based on a structural alignment, all but one of the RpfB residues that contact NAG_3 are conserved in RpfE [Fig. 2(B)]. RpfB Gly350, however, is replaced in RpfE by Arg163. This residue overlaps with superimposed NAG_3, requiring conformational adjustments for substrate binding [Fig. 2(C)].

Importantly, the calculated surface potential of RpfE is more basic than that of RpfB in the predicted binding sites for the isoglutamate residue in both interacting peptide crosslinks in bound PG [Fig. 1(C)]. This charge reversal in RpfE compared to RpfB is positioned to complement isoglutamate (RpfE) or isoglutamine (RpfB) in the modeled crosslinks. The sequence variation in the predicted peptide binding groove is observed not only among Rpfs in *Mtb*, but also in the three homologs in the simplified genome of *Mycobacterium leprae*[18] [Fig. 3(A–C)]. Because the genome of *M. leprae* has suffered mutations that inactivate all but the most important genes, the conservation of charge reversal in the predicted peptide-crosslink interacting surfaces of the Rpfs supports the potential functional importance of Rpf proteins capable of discriminating between modifications in the peptide moieties in PG.

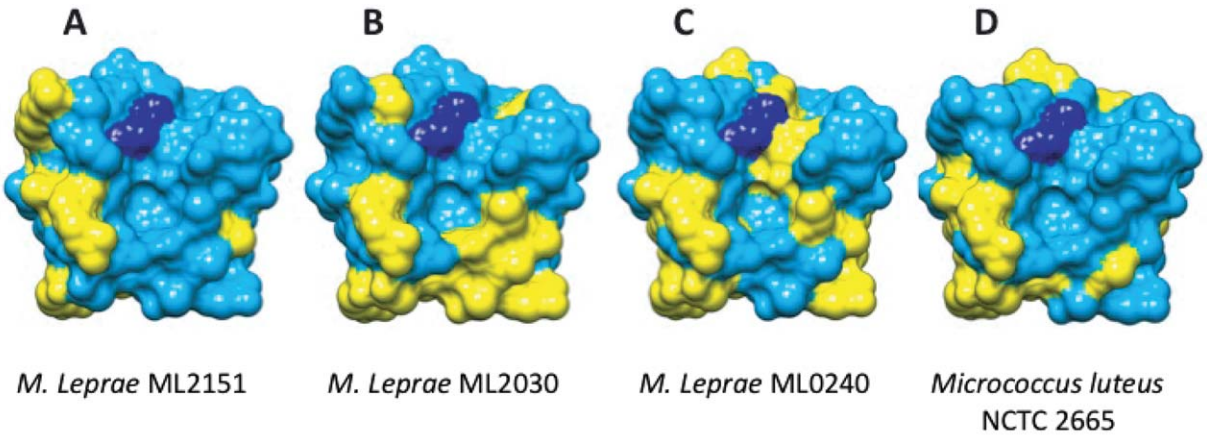

E

```
                          100       110       120       130       140       150       160       170
                          .         .         .         .         .         .         .         .
Mtb RpfE                  NWDAIAQCESGGNWSINTGNGYYGGLRFTAGTWRANGG...SGSAANASREEQIRVAENVLRSQGIRAWPVC.GRRG
Mtb RpfB                  .WDAIAQCESGGNWSINTGNGYYGGLRFTAGTWRANGG---SGSAANASREEQIRVAENVLRSQGIRAWPVC.GRR.
M. leprae ML2151          EWDQVARCESGGNWSINTGNGYLGGLQFSQGTWASHGGGEYAPSAQLATREQQIAVAERVLATQGSGAWPACGH...
M. leprae ML2030          NWDAVAQCESGRNWRANTGNGFYGGLQFKPTIWARYGG...VGNPAGASREQQITVANRVLADQGLDAWPKCG....
M. Leprae ML0240          .WDAIAGCEAGGNWAINTGNGYYGGVQFDQGTWVANGGLRYAPRADLATREEQIAVAEVTRARQGWDAWPVCSGRVG
M. Luteus NCTC 2665       TWDRLAECESNGTWDINTGNGFYGGVQFTLSSWQAVGG...EGYPHQASKAEQIKRAEILQDLQGWGAWPLC.SQK.
```

Figure 3. Sequence variation for RpfE and *Mycobacterium leprae* homologs. Conserved (blue) and variable residues (yellow) in RpfE and ML2151, ML2030, and ML0240, respectively, (A), (B), and (C). Sequence differences are prominent in the predicted peptide-binding groove to the right of the catalytic glutamate (dark blue) and the predicted carbohydrate-binding surface below the active-site pocket. D: Sequence variation between RpfE and the most similar protein in *Micrococcus luteus* (51% sequence identity) shows homologies in a more distantly related Rpf. E: Sequence aligment of *Mtb* RpfE and RpfB catalytic domain with *M. leprae* and *M. luteus* Rpfs.

The specialization of Rpf proteins

The unique roles of Rpf proteins in bacteria have not yet been elucidated. Among the five *Mtb* Rpf proteins, the transglycosylase domain is conserved, but the presence of additional domains is predicted to impart different functions. In addition, a prevalent idea is that Rpf genes are regulated independently by distinct mechanisms. Moreover, Rpf proteins may be regulated by association with distinct partners. Rubin and coworkers[10,11] reported the interaction between RpfB/E and RipA, a peptidase involved in PG remodeling and cell division. The nature of the interaction is uncertain, however, because the structure of RipA[19] revealed that most of the putative Rpf-interacting segment identified using a yeast two-hybrid assay forms a buried β-strand. Nonetheless, a PG fragment released by the action of a hydrolase (Rpf) and the essential peptidase, RipA, is a likely candidate for signaling cell reactivation. The work presented here, describing the structure of an *Mtb* Rpf protein, reveals structural and chemical differences of the catalytic cleft that may enable recognition of variations in PG or reactions with different pH optima. Overall, specialization in appended domains, gene expression, enzyme regulation, and chemical specificity may contribute to the functional differences among Rpfs.

Materials and Methods

RpfE catalytic domain cloning expression and purification

Nucleotide sequence corresponding to the RpfE catalytic domain (98–172) was amplified by PCR using H37Rv genomic DNA. The PCR product was cloned in a HisMBP expression vector (2MT vector http://www.addgene.org), carrying a tobacco etch virus (TEV) protease cleavage site at the N-terminus of RpfE. The protein was expressed using the Rosetta2(DE3)pLysS expression system (Novagen). Cells were grown at 37°C until optical density $(OD)_{600}$ 0.6 was reached, and cultures were induced with 1 m*M* isopropyl β-D-1-thiogalactopyranoside (IPTG) at 16°C and shaken overnight for protein expression. The cell pellets were resuspended in Buffer A (300 m*M* NaCl, 20 m*M* imidazole, 20 m*M* Tris pH 8, 10% glycerol, 0.5 m*M* (tris(2-carboxyethyl)phosphine) (TCEP)), containing protease inhibitor cocktails (E-64, leupeptin, and AEBSF). The cells were sonicated on ice and the lysate centrifuged at 18,000 rpm for 1 h. Supernatant was loaded onto a Ni-affinity column

and washed with 10 volumes of Buffer A. The protein was eluted with Buffer B (300 m*M* NaCl, 20 m*M* Tris pH 8, 0.5 m*M* TCEP, 300 m*M* imidazole, 10% glycerol). TEV protease was added, and the protein was dialyzed against Buffer A (without TCEP) overnight to remove the excess of imidazole. In the same dialysis buffer, a 10:1 ratio of reduced glutathione (10 m*M*) versus oxidized glutathione (1 m*M*) was added to promote formation of disulfide bonds.[20] The reaction mixture was purified by an additional affinity chromatography step on a Ni column to remove the His_MBP tag and TEV protease. The flow-through fraction was concentrated and further purified on a preparative HiLoad 26/60 Superdex 75 column (GE) in Buffer C (100 m*M* NaCl, 5% glycerol, and 20 m*M* Tris pH 8), where RpfE ran as a monomer. Elution fractions were collected and investigated by Coomassie blue-stained SDS PAGE.

RpfE crystallization, data collection and structure determination

The fractions containing RpfE were concentrated to 12 mg/mL, and the protein was screened for crystallization by hanging drop vapor diffusion. RpfE crystallized as small needles in more than 70% of screened conditions.

Several crystals generated in different conditions were screened for diffraction. Crystals that grew in 25% polyethylene glycol (PEG) 3350, 0.1*M* (4-(2-hydroxyethyl)-1-piperazineethanesulfonic acid) (HEPES) sodium pH 6.8, in the presence of Silver Bullets HT F1 condition (0.25% wt/vol methylenediphosphonic acid, 0.25% wt/vol Phytic acid sodium salt hydrate, 0.25% wt/vol sodium pyrophosphate tetrabasic decahydrate, 0.25% wt/vol sodium triphosphate pentabasic, 0.02*M* HEPES sodium pH 6.8) provided the best diffraction data. Crystals were frozen using 25% PEG 3350, 0.1*M* HEPES sodium, and 10% PEG 200 as cryoprotectant. Diffraction data were collected at the Lawrence Berkeley National Laboratory Advanced Light Source Beamline 8.3.1.[21] Data were scaled using HKL2000. The PHENIX software suite[22] was used for model building by molecular replacement using the RpfB homolog (3EO5 in PDB) as the search model. Cycles of refinement were performed with PHENIX. Images and structural alignments were generated using Chimera software.[23] Protein surface potential was calculated using Swiss-PdbViewer.

Coordinates

The coordinates and structure factors were deposited in the PDB under the accession number 4CGE.

Acknowledgments

Authors thank J. Holton, G. Meigs, and J. Tanamachi at Beamline 8.3.1 at Lawrence Berkeley National Laboratory for help with X-ray data collection. They also thank Abbey Hartland and Scott Gradia from the QB3 Macrolab at University of California, Berkeley. Authors appreciate the support of the TB Structural Genomics Consortium (NIH grant P01 AI068135-06). The authors declare no conflict of interest.

References

1. Loddenkemper R, Hauer B (2010) Drug-resistant tuberculosis: a worldwide epidemic poses a new challenge. Dtsch Arztebl Int 107:10–19.
2. Russell-Goldman E, Xu J, Wang X, Chan J, Tufariello JM (2008) A *Mycobacterium tuberculosis* Rpf double-knockout strain exhibits profound defects in reactivation from chronic tuberculosis and innate immunity phenotypes. Infect Immun 76:4269–4281.
3. Tufariello JM, Mi K, Xu J, Manabe YC, Kesavan AK, Drumm J, Tanaka K, Jacobs WR, Jr, Chan J (2006) Deletion of the *Mycobacterium tuberculosis* resuscitation-promoting factor Rv1009 gene results in delayed reactivation from chronic tuberculosis. Infect Immun 74:2985–2995.
4. Gupta RK, Srivastava R (2012) Resuscitation promoting factors: a family of microbial proteins in survival and resuscitation of dormant mycobacteria. Indian J Microbiol 52:114–121.
5. Holtje JV (1996) Lytic transglycosylases. EXS 75:425–429.
6. Cohen-Gonsaud M, Barthe P, Bagneris C, Henderson, B, Ward J, Roumestand C, Keep NH (2005) The structure of a resuscitation-promoting factor domain from *Mycobacterium tuberculosis* shows homology to lysozymes. Nat Struct Mol Biol 12:270–273.
7. Ruggiero A, Tizzano B, Pedone E, Pedone C, Wilmanns M, Berisio R (2009) Crystal structure of the resuscitation-promoting factor (DeltaDUF)RpfB from *M. tuberculosis*. J Mol Biol 385:153–162.
8. Alber T (2009) Signaling mechanisms of the *Mycobacterium tuberculosis* receptor Ser/Thr protein kinases. Curr Opin Struct Biol 19:650–657.
9. Kana BD, Mizrahi V (2010) Resuscitation-promoting factors as lytic enzymes for bacterial growth and signaling. FEMS Immunol Med Microbiol 58:39–50.
10. Hett EC, Chao MC, Deng LL, Rubin EJ (2008) A mycobacterial enzyme essential for cell division synergizes with resuscitation-promoting factor. PLoS Pathog 4:e1000001.
11. Hett EC, Chao MC, Steyn AJ, Fortune SM, Deng LL, Rubin EJ (2007) A partner for the resuscitation-promoting factors of *Mycobacterium tuberculosis*. Mol Microbiol 66:658–668.
12. Cole ST, Brosch R, Parkhill J, Garnier T, Churcher C, Harris D, Gordon SV, Eiglmeier K, Gas S, Barry CE, III, Tekaia F, Badcock K, Basham D, Brown D, Chillingworth T, Connor R, Davies R, Devlin K, Feltwell T, Gentles S, Hamlin N, Holroyd S, Hornsby T, Jagels K, Krogh A, McLean J, Moule S, Murphy L, Oliver K, Osborne J, Quail MA, Rajandream MA, Rogers J, Rutter S, Seeger K, Skelton J, Squares R, Squares S, Sulston JE, Taylor K, Whitehead S, Barrell BG (1998) Deciphering the biology of *Mycobacterium tuberculosis* from the complete genome sequence. Nature 393:537–544.
13. Kana BD, Gordhan BG, Downing KJ, Sung N, Vostroktunova G, Machowski EE, Tsenova L, Young M, Kaprelyants A, Kaplan G, Mizrahi V (2008) The resuscitation-promoting factors of *Mycobacterium tuberculosis* are required for virulence and

resuscitation from dormancy but are collectively dispensable for growth in vitro. Mol Microbiol 67:672–684.
14. Tufariello JM, Jacobs WR, Jr, Chan J (2004) Individual *Mycobacterium tuberculosis* resuscitation-promoting factor homologues are dispensable for growth in vitro and in vivo. Infect Immun 72:515–526.
15. Beste DJ, Espasa M, Bonde B, Kierzek AM, Stewart GR, McFadden J (2009) The genetic requirements for fast and slow growth in mycobacteria. PLoS One 4: e5349.
16. Squeglia F, Romano M, Ruggiero A, Vitagliano L, De Simone A, Berisio R (2013) Carbohydrate recognition by RpfB from *Mycobacterium tuberculosis* unveiled by crystallographic and molecular dynamics analyses. Biophys J 104:2530–2539.
17. Hett EC, Rubin EJ (2008) Bacterial growth and cell division: a mycobacterial perspective. Microbiol Mol Biol Rev 72:126–156.
18. Cole ST, Eiglmeier K, Parkhill J, James KD, Thomson NR, Wheeler PR, Honore N, Garnier T, Churcher C, Harris D, Mungall K, Basham D, Brown D, Chillingworth T, Connor R, Davies RM, Devlin K, Duthoy S, Feltwell T, Fraser A, Hamlin N, Holroyd S, Hornsby T, Jagels K, Lacroix C, Maclean J, Moule S, Murphy L, Oliver K, Quail MA, Rajandream MA, Rutherford KM, Rutter S, Seeger K, Simon S, Simmonds M, Skelton J, Squares R, Squares S, Stevens K, Taylor K, Whitehead S, Woodward JR, Barrell BG (2001) Massive gene decay in the leprosy bacillus. Nature 409:1007–1011.
19. Ruggiero A, Marasco D, Squeglia F, Soldini S, Pedone E, Pedone C, Berisio R (2010) Structure and functional regulation of RipA, a mycobacterial enzyme essential for daughter cell separation. Structure 18:1184–1190.
20. Annis I, Hargittai B, Barany G (1997) Disulfide bond formation in peptides. Methods Enzymol 289:198–221.
21. MacDowell AA, Celestre RS, Howells M, McKinney W, Krupnick J, Cambie D, Domning EE, Duarte RM, Kelez N, Plate DW, Cork CW, Earnest TN, Dickert J, Meigs G, Ralston C, Holton JM, Alber T, Berger JM, Agard DA, Padmore HA (2004) Suite of three protein crystallography beamlines with single superconducting bend magnet as the source. J Synchrotron Radiat 11: 447–455.
22. Adams PD, Afonine PV, Bunkoczi G, Chen VB, Davis IW, Echols N, Headd JJ, Hung LW, Kapral GJ, Grosse-Kunstleve RW, McCoy AJ, Moriarty NW, Oeffner R, Read RJ, Richardson DC, Richardson JS, Terwilliger TC, Zwart PH (2010) PHENIX: a comprehensive Python-based system for macromolecular structure solution. Acta Cryst D 66:213–221.
23. Pettersen EF, Goddard TD, Huang CC, Couch GS, Greenblatt DM, Meng EC, Ferrin TE (2004) UCSF Chimera—a visualization system for exploratory research and analysis. J Comput Chem 25:1605–1612.